

# Proton-Transfer Reactions between Nitroalkanes and Hydroxide Ion under Non-Steady-State Conditions. Apparent and Real Kinetic Isotope Effects

Yixing Zhao, Yun Lu, and Vernon D. Parker\*

Contribution from the Department of Chemistry and Biochemistry, Utah State University, Logan, Utah 84322-0300

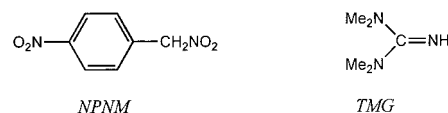
Received October 5, 2000

**Abstract:** The kinetics of the proton-transfer reactions between 1-nitro-1-(4-nitrophenyl)ethane (NNPE<sub>H(D)</sub>) and hydroxide ion in water/acetonitrile (50/50 vol %) were studied at temperatures ranging from 289 to 319 K. The equilibrium constants for the reactions are large under these conditions, ensuring that the back reaction is not significant. The extent of reaction/time profiles during the first half-lives are compared with theoretical data for the simple single-step mechanism and a 2-step mechanism involving initial donor/acceptor complex formation followed by unimolecular proton transfer and dissociation of ions. In all cases, the profiles for the reactions of both NNPE<sub>H</sub> and NNPE<sub>D</sub> deviate significantly from those expected for the simple single-step mechanism. Excellent fits of experimental data with theoretical data for the complex mechanism, in the pre-steady-state time period, were observed in all cases. At all base concentrations (0.5 to 5.0 mM) and at all temperatures the apparent kinetic isotope effects (KIE<sub>app</sub>) were observed to increase with increasing extent of reaction. Resolution of the kinetics into microscopic rate constants at 298 K resulted in a real kinetic isotope effect (KIE<sub>real</sub>) for the proton-transfer step equal to 22. Significant proton tunneling was further indicated by the temperature dependence of the rate constants for proton and deuterium transfers: KIE<sub>real</sub> ranging from 17 to 26,  $E_a^D - E_a^H$  equal 2.8 kcal/mol, and  $A^D/A^H$  equal to 4.95.

Numerous studies of the proton-transfer reactions of nitroalkanes with both neutral and anionic bases have been carried out over the past half-century.<sup>1–25</sup> The reactions are conveniently studied by spectrophotometry since the stable anionic products

- (1) Caldin, E. F.; Trickett, J. C. *Trans. Faraday Soc.* **1953**, *49*, 772.
- (2) Lewis, E. S.; Funderburk, L. H. *J. Am. Chem. Soc.* **1967**, *89*, 2322.
- (3) Bordwell, F. G.; Boyle, W. J.; Yee, K. C. *J. Am. Chem. Soc.* **1970**, *92*, 5926.
- (4) Caldin, E. F.; Jarczewski, A.; Leffek, K. T. *Trans. Faraday Soc.* **1971**, *67*, 110.
- (5) Jarczewski, A.; Leffek, K. T. *Can. J. Chem.* **1972**, *50*, 24.
- (6) Kim, J.-H.; Leffek, K. T. *Can. J. Chem.* **1974**, *52*, 592.
- (7) Caldin, E. F.; Mateo, S. *Chem. Commun.* **1973**, 854.
- (8) Caldin, E. F.; Mateo, S. *J. Chem. Soc., Faraday Trans. 1* **1975**, *71*, 1876.
- (9) Jarczewski, A.; Pruszyński, P. *Can. J. Chem.* **1975**, *53*, 1176.
- (10) Caldin, E. F.; Dawson, E.; Hyde, R. M. *J. Chem. Soc., Faraday Trans. 1* **1975**, *71*, 528.
- (11) Bordwell, F. G.; Boyle, W. J. *J. Am. Chem. Soc.* **1975**, *97*, 3447.
- (12) Rogne, O. *Acta Chem. Scand.* **1978**, 559.
- (13) Jarczewski, A.; Pruszyński, P.; Leffek, K. T. *Can. J. Chem.* **1979**, *57*, 669.
- (14) Kresge, A. J.; Powell, M. F. *J. Am. Chem. Soc.* **1981**, *103*, 201.
- (15) Caldin, E. F.; Mateo, S.; Warrick, P. *J. Am. Chem. Soc.* **1981**, *103*, 202.
- (16) Sugimoto, N.; Sasaki, M.; Osugi, J. *J. Phys. Chem.* **1982**, *86*, 3418.
- (17) Jarczewski, A.; Pruszyński, P.; Leffek, K. T. *Can. J. Chem.* **1983**, *61*, 2029.
- (18) Sugimoto, N.; Sasaki, M.; Osugi, J. *Bull. Chem. Soc. Jpn.* **1984**, *57*, 366.
- (19) Pruszyński, P.; Jarczewski, A. *J. Chem. Soc., Perkin Trans. 2* **1986**, 1117.
- (20) Leffek, K. T.; Pruszyński, P. *Can. J. Chem.* **1988**, *66*, 1454.
- (21) Galezowski, W.; Jarczewski, A. *J. Chem. Soc., Perkin Trans. 2* **1989**, 1647.
- (22) Leffek, K. T.; Pruszyński, P.; Thanapaalasingham, K. *Can. J. Chem.* **1989**, *67*, 590.
- (23) Kresge, A. J.; Powell, M. F. *J. Phys. Org. Chem.* **1990**, *3*, 55.
- (24) Galezowski, W.; Jarczewski, A. *Can. J. Chem.* **1990**, *68*, 2242.

exhibit strong absorbance bands in the visible spectral region. The very large deuterium kinetic isotope effects ( $\cong 50$ ) reported by Caldin and Mateo<sup>7,8</sup> for the reaction between 4-nitrophenylnitromethane (NPNM) with tetramethylguanidine (TMG), a strong organic base with an exchangeable N–H, in toluene were quickly challenged by two groups.<sup>12,14,23</sup> Reinvestigations of the



reaction revealed that the results reported for the D-labeled acid are unreliable due to proton/deuteron (H/D) exchange and that KIE<sub>app</sub> was lowered to about 11 when the base was changed to (Me<sub>2</sub>N)<sub>2</sub>C=ND.

There have been no suggestions of kinetically important intermediates in these reactions; all discussions have considered the reactions as simple second-order equilibria (eq 1). We have recently observed that the proton-transfer reactions of some organic



radical cations<sup>26</sup> follow a mechanism involving prior formation of a kinetically significant radical cation/base complex before irreversible proton transfer. Two characteristic features of kinetic data obtained in the time period before steady-state is reached were reported for this mechanism. These include (a) the extent

(25) Jarczewski, A.; Schroeder, G.; Leffek, K. T. *Can. J. Chem.* **1991**, *69*, 468.

(26) Parker, V. D.; Zhao, Y.; Lu, Y.; Zheng, G. *J. Am. Chem. Soc.* **1998**, *120*, 12720.

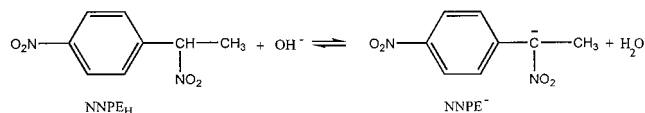
of reaction–time profiles that are distinctly different than expected for the simple second-order mechanism and (b) apparent kinetic isotope effects ( $KIE_{app}$ ) which vary significantly with the extent of reaction in that time period.

We considered it likely that the proton-transfer reactions of nitroalkanes with bases might follow a similar 2-step mechanism. As pointed out earlier, there has been some confusion regarding the magnitude of deuterium kinetic isotope effects for these reactions. The factor responsible for this situation is that if the reverse reaction is significant, H/D exchange takes place which complicates the determination of the rate constant for deuterium transfer of the isotopically labeled acid. The best way to avoid this complication is to study reactions which lie far to the right thus ensuring that the reverse reaction is insignificant. The reaction between 1-nitro-1-(4-nitrophenyl)ethane ( $NNPE_H$ ) and hydroxide ion appeared to fit this criterion. The  $pK_a$  values of  $NNPE_H$  in water and in water/methanol (50/50 vol %) have been reported to be 6.5<sup>11</sup> and 7.5<sup>3</sup>, respectively. These values correspond to equilibrium constants of the order of  $>10^8$  for the proton-transfer reactions between  $NNPE_H$  and hydroxide ion in these solvents and we concluded that isotopic exchange should not significantly affect deuterium kinetic isotope effect measurements.

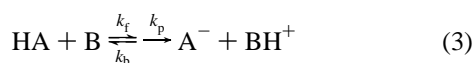
We have found that the formation of the conjugate base ( $NNPE^-$ ) during the pre-steady-state period in the reaction between  $NNPE_{H(D)}$  and hydroxide ion can be monitored by stopped-flow spectrophotometry. The results of the kinetic studies discussed here strongly support the hypothesis of a 2-step mechanism for this reaction.

## Results

The reaction between  $NNPE_H$  and hydroxide ion in aqueous solvents is illustrated below. The features of this reaction which make it suitable for detailed kinetic analysis are (a) the equilibrium constant for the reaction is of the order of  $>10^8$  which eliminates complications due to the reverse reaction (data in Table 3 discussed later), (b) the anionic product of the reaction ( $NNPE^-$ ) is stable and readily monitored by spectrophotometry, and (c) the proton removed is at a tertiary position which avoids possible isotope effect complications due to secondary  $\alpha$ -hydrogens.



**Protocol for Distinguishing between Single-Step and Two-Step Proton-Transfer Mechanisms.** For the time being we will consider thermodynamically favorable proton-transfer reactions in which the reverse reactions can be neglected. The two mechanisms under these conditions are shown in eqs 2 and 3.



Once steady state is reached for the 2-step mechanism 3, which involves the formation of a kinetically significant intermediate, the rate laws for the two mechanisms differ only by the definition of the apparent rate constant ( $k_{app}$ ). For the 1-step mechanism  $k_{app}$  is equal to the microscopic rate constant for reaction 2 and is given for mechanism 3 by the steady-state expression 4. In the time period before steady state is achieved

$$d[\text{A}^-]/dt = k_{app}[\text{HA}][\text{B}]; \quad [k_{app} = (k_f)(k_p)/(k_p + k_b)] \quad (4)$$

the various rate constants affect the overall reaction rate to different degrees than implied by rate law 4 and the concentration–time profiles of the anionic product ( $\text{A}^-$ ) can differ significantly for the two mechanisms. The ratio of the time necessary for the extent of reaction to equal 0.50 to that necessary for the extent of reaction to equal 0.05 ( $t_{0.5}/t_{0.05}$ ) is a convenient indicator of deviations of kinetic data from that expected for the simple 1-step mechanism. For reaction 2, under pseudo-first-order conditions (large excess of B), this ratio is equal to 13.5 while under the same conditions for reaction 3 the ratio is dependent upon the magnitudes of the rate constants ( $k_f$ ,  $k_p$ , and  $k_b$ ). Calculations using the integrated rate equation for the pseudo-first-order version of reaction 3 show that the ratio can be significantly lower than 13.5, which is the limiting maximum value for this mechanism. Under second-order conditions, the ratio ( $t_{0.5}/t_{0.05}$ ) for reaction 2 is larger than 13.5 and varies with the concentrations of reactants.

Another significant difference in kinetic data for mechanisms 2 and 3 is the dependence or the absence of a dependence of the apparent deuterium kinetic isotope effect ( $KIE_{app}$ ) on the extent of reaction. For the single-step mechanism  $KIE_{app}$  is always expected to be the real value ( $KIE_{real}$ ) and independent of the extent of reaction. The situation is considerably more complex for the 2-step mechanism. After steady state is reached, the two mechanisms are kinetically indistinguishable. On the other hand, in the time period before steady state is reached for the 2-step mechanism,  $KIE_{app}$  can change significantly with changes in the extent of reaction. This phenomenon was first demonstrated for the reactions of methylarene radical cations with pyridine bases.<sup>26</sup>

**Extent of Reaction–Time Profiles for the Reactions between  $NNPE_H$  and Hydroxide Ion.** The extent of reaction–time profiles shown in Figure 1 are for the reactions of  $NNPE_H$  (0.1 mM) with hydroxide ion (concentrations ranging from 0.5 to 5.0 mM) in water/acetonitrile (50/50 vol %) at 298.3 K. The experimental data are the solid squares while the responses expected for the simple single-step mechanism are indicated by the dashed lines. At all base concentrations, the experimental data deviate significantly from that expected for the single-step mechanism. The theoretical values of the ratio ( $t_{0.5}/t_{0.05}$ ) for the 1-step mechanism are 14.3 (0.5 mM), 13.9 (1.0 mM), 13.7 (2.0 mM), and 13.6 (5.0 mM) while the corresponding experimental values observed were 12.6, 12.4, 12.3, and 12.3, respectively.

**Apparent Deuterium Kinetic Isotope Effects.** Kinetic experiments carried out with  $NNPE_D$  (1-nitro-1-(4-nitrophenyl)ethane-*d*<sub>1</sub>) under the same conditions as described in the previous section resulted in the extent of reaction–time profiles illustrated in Figure 2. Apparent deuterium kinetic isotope effects as a function of the extent of reaction were calculated from the corresponding ratios of times observed for the reactions of  $NNPE_D$  and  $NNPE_H$  ( $t_D/t_H$ ). The ranges of  $KIE_{app}$  observed were (7.13–7.54), (7.13–7.45), (7.06–7.48), and (7.11–7.53) for reactions with hydroxide concentrations of 0.5, 1.0, 2.0, and 5.0 mM, respectively.

**Fitting Experimental to Theoretical Extent of Reaction–Time Data for the 2-Step Mechanism.** The extent of reaction–time curves for the reactions of  $NNPE_H$  (Figure 1) and  $NNPE_D$  (Figure 2) with hydroxide ion can readily be fit with theoretical data for the 2-step proton-transfer mechanism. Considering only the  $NNPE_H$  or the  $NNPE_D$  data separately, however, does not result in unique fits of experimental to theoretical data. There are a number of different combinations of rate constants ( $k_f$ ,  $k_b$ ,

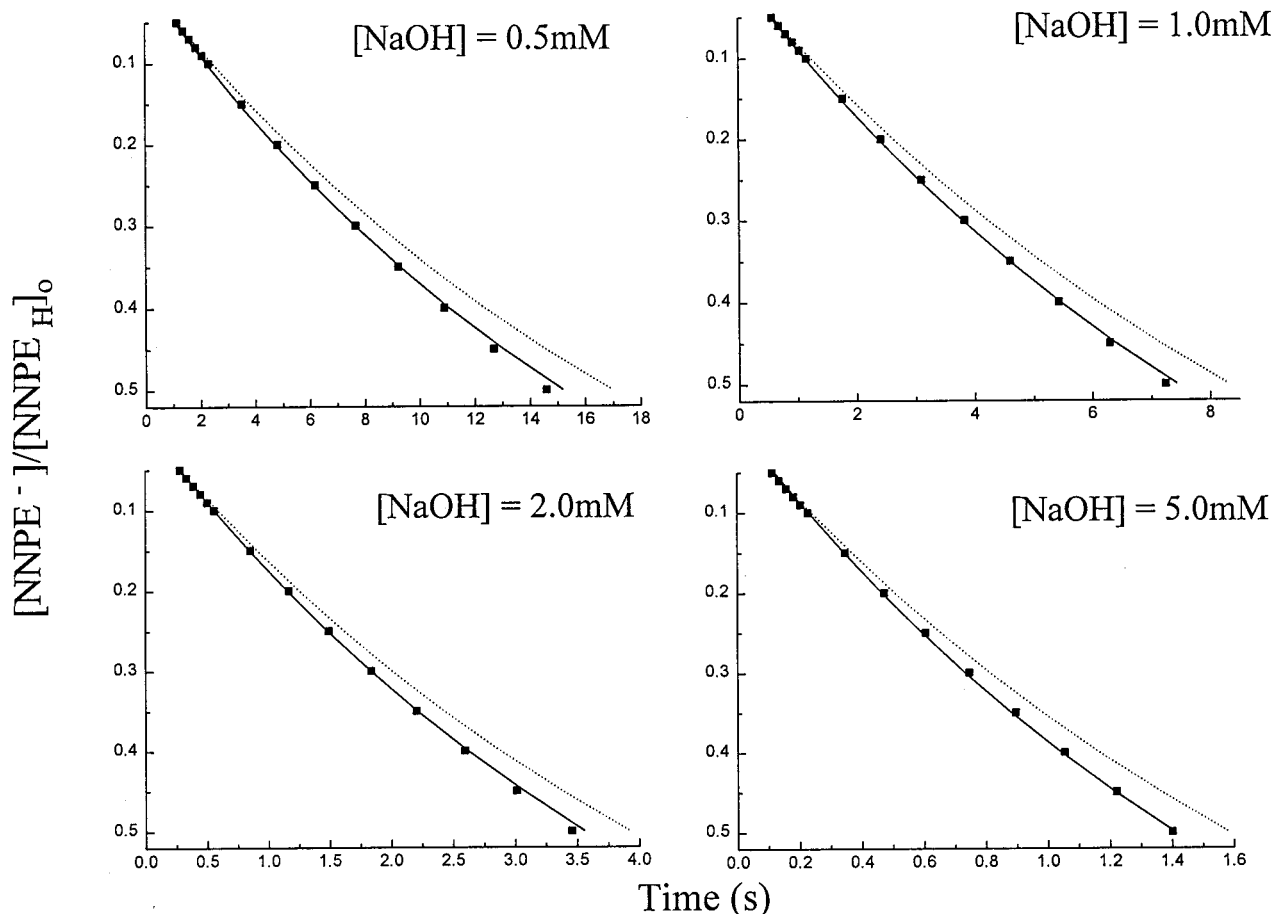


**Figure 1.** Extent of reaction–time profiles for the reactions of NNPE<sub>H</sub> (0.1 mM) with hydroxide ion (concentrations given on the plots): experimental data, solid squares; theoretical data for the 1-step mechanism, dashed lines; theoretical data for the 2-step mechanism, solid lines.

and  $k_p$ ) which give acceptable fits for any one extent of reaction–time profile. We have previously shown that a unique fit of experimental to theoretical data for the 2-step mechanism can be achieved by concurrent fitting of data for both HA and DA (NNPE<sub>H</sub> and NNPE<sub>D</sub> in the present case).<sup>26</sup> The latter involves the assumption that  $k_f$  and  $k_b$  are not affected by the isotopic change while the rate constants for the proton and deuteron transfer steps ( $k_p^H$  and  $k_p^D$ , respectively) differ significantly.

In addition to the extent of reaction–time profiles, the experimental data include the apparent steady-state rate constants for the reactions of HA [ $(k_{app}^H)_{ss}$ ] and DA [ $(k_{app}^D)_{ss}$ ]. The expressions for the steady-state rate constants can be rearranged to give eqs 5 and 6,

$$(k_{app}^H)_{ss}/k_f = (k_p^H/k_b)/(1 + k_p^H/k_b) = CH \quad (5)$$

$$(k_{app}^D)_{ss}/k_f = (k_p^D/k_b)/(1 + k_p^D/k_b) = CD \quad (6)$$

which result in eq 7 for the real kinetic isotope effect,  $KIE_{real}$ . Thus, in addition to the apparent rate constants, it is only necessary to determine  $k_f$  in order to evaluate  $KIE_{real}$ .

$$KIE_{real} = k_p^H/k_p^D = [CH/(1 - CH)]/[CD/(1 - CD)] \quad (7)$$

Theoretical data for the 2-step mechanism were obtained either by using the integrated rate law (pseudo-first-order conditions) or by 4th order Runge–Kutta numerical integration (second-order conditions).<sup>27</sup> No significant differences were observed in data obtained by both methods. A brief description,

based on the published procedure,<sup>26</sup> of the data-fitting procedure can be found in the Experimental Section.

**The Effect of Base Concentration on Kinetic Data for the Reactions of NNPE<sub>H</sub> and NNPE<sub>D</sub> in Water/Acetonitrile (50/50 vol %).** The solid lines in Figures 1 and 2 are theoretical data for mechanism 3 with the following rate constants:  $k_f$  (139 M<sup>-1</sup> s<sup>-1</sup>),  $k_b$  (12.6 ± 0.4 s<sup>-1</sup>),  $k_p^H$  (28.2 s<sup>-1</sup>), and  $k_p^D$  (1.26 ± 0.06 s<sup>-1</sup>). The reason for the range of values for  $k_b$  and  $k_p^D$  is that these rate constants were evaluated using eqs 3–6 and small variations were observed in the apparent steady-state rate constants. All of the data resulting from the analyses with hydroxide concentrations ranging from 0.5 to 5.0 mM are summarized in Table 1.

**The Effect of Temperature on Kinetic Parameters for the Reactions of NNPE<sub>H</sub> and NNPE<sub>D</sub> with Hydroxide Ion in Water/Acetonitrile (50/50 vol %).** Plots of extent of reaction–time data for the reactions of NNPE<sub>H</sub> (0.1 mM) and NNPE<sub>D</sub> (0.1 mM) with hydroxide ion (2.0 mM) at temperatures ranging from 288.8 to 319.2 K are shown in Figures 3 and 4, respectively. The solid squares are the experimental data, the dashed lines are theoretical data for the 1-step mechanism, and the solid lines are theoretical data for the 2-step mechanism. In all cases, the experimental data deviate significantly from that expected for the simple 1-step mechanism and very good experimental to theoretical data fits are obtained for the 2-step mechanism. The various rate constants and kinetic isotope effect data are summarized in Table 2. Arrhenius plots for  $k_{app}^H$ ,  $k_{app}^D$ ,  $k_p^H$ , and  $k_p^D$  are illustrated in Figure 5.

(27) For a recent discussion of methods to analyze complex reactions see ref 28.

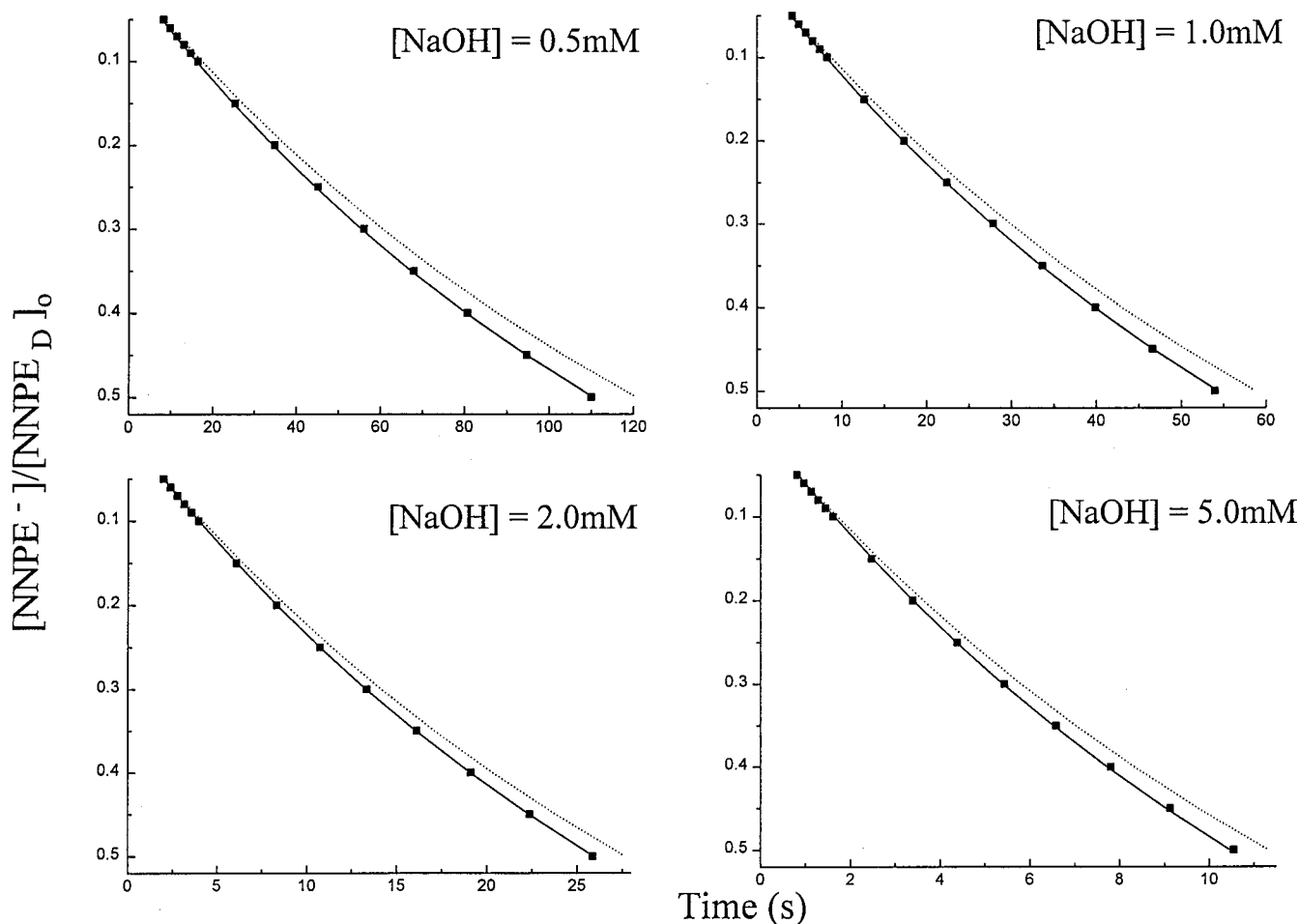


**Figure 2.** Extent of reaction–time profiles for the reactions of  $\text{NNPE}_D$  (0.1 mM) with hydroxide ion (concentrations given on the plots): experimental data, solid squares; theoretical data for the 1-step mechanism, dashed lines; theoretical data for the 2-step mechanism, solid lines.

**Table 1.** Rate Constants for Proton and Deuteron Transfer Reactions of  $\text{NNPE}_{H(D)}$  (0.1 mM) with NaOH in Water/Acetonitrile (50:50 vol %) at 298.3 K<sup>a</sup>

NaOH (mM)	$k_{\text{app}}^H$	$k_{\text{app}}^D$	$k_f$	$k_p^H$	$k_p^D$	$k_b$	$\text{KIE}_{\text{app}}$	$\text{KIE}_{\text{real}}$
0.5	97.0	13.4	139	28.2	1.31	12.2	7.14–7.53	21.6
1.0	96.5	13.3	139	28.2	1.31	12.4	7.02–7.38	21.5
2.0	99.8	13.9	139	28.2	1.23	11.1	7.06–7.48	22.9
5.0	101	14.0	139	28.2	1.19	10.6	7.11–7.53	23.6

<sup>a</sup> Units: second-order rate constants ( $k_{\text{app}}^H$ ,  $k_{\text{app}}^D$ ,  $k_f$ ) are in  $\text{M}^{-1} \text{s}^{-1}$  and first-order rate constants ( $k_p^H$ ,  $k_p^D$ ,  $k_b$ ) are in  $\text{s}^{-1}$ .

**The Effect of the Reverse Reaction on Extent of Reaction–Time Profiles for the Single-Step Proton-Transfer Reaction.** Although it is well-known that H/D exchange<sup>12,14,23</sup> causes uncertainty in deuterium kinetic isotope effect measurements, there are no data available which may be used to predict the effect on the extent of reaction–time profiles. The data in Table 3 were calculated for the general reversible proton-transfer reaction 1. To mimic our experiments, the initial concentration of acid  $[\text{HA}]_0$  was set at 0.0001 M and that for the base  $[\text{B}]_0$  was taken to equal 0.005 M while that of the conjugate acid of B,  $[\text{HB}^+]_0$ , was set equal to 55.6. The time ratios,  $(t_{0.50}/t_{0.05})_H$  and  $(t_{0.50}/t_{0.05})_D$ , were chosen to demonstrate the effect of the equilibrium on theoretical data for the reactions of HA and the effects of both equilibrium and exchange on that for the reactions of DA. The rate constants used in the calculations were  $100 \text{ M}^{-1} \text{ s}^{-1}$  for the forward reaction of HA and  $10 \text{ M}^{-1} \text{ s}^{-1}$  for the forward reaction of DA. The rate constant for the reverse reaction, which was taken to be the same for both HA and DA,

was varied to show the effect of the equilibrium constant ( $K_{\text{equil}}$ ) on the kinetic data. The data show that as long as the equilibrium constant is  $10^6$  or greater, where the extent of reaction at equilibrium is 0.989 or greater, the time ratios are not significantly different from 13.5, that for the irreversible single-step mechanism. At lower values of  $K_{\text{equil}}$  both  $(t_{0.50}/t_{0.05})_H$  and  $(t_{0.50}/t_{0.05})_D$  increase markedly with decreases in  $K_{\text{equil}}$ . The deviations for the former are due to the reversibility of the reaction while that for the latter reflect both the reversibility and H/D exchange. (The back reaction for both HA and DA was assumed to be  $\text{A}^- + \text{BH}^+ \rightarrow \text{HA} + \text{B}$ .)

**The Effect of a Nonproductive Equilibrium on Extent of Reaction–Time Profiles for the Single-Step Proton-Transfer Reaction.** It is clear that a nonproductive equilibrium involving the reactants will affect the extent of reaction–time profiles for the single-step proton-transfer reaction. To determine the manner in which kinetic data are affected by this situation, the data in Table 4 were calculated for an irreversible proton-transfer reaction accompanied by a nonproductive equilibrium ( $\text{HA} + \text{B} = \text{complex}$ ) that is not on the pathway to products. The rate constant for the proton-transfer reaction ( $k_{\text{productive}}$ ) was set at  $1 \text{ M}^{-1} \text{ s}^{-1}$  and the rate constants for the equilibrium ( $k_f$  (nonproductive) and  $k_b$  (nonproductive)) were varied as shown in Table 4. The data show that the effect of the nonproductive equilibrium is to cause  $(t_{0.50}/t_{0.05})$  to be greater than that for the simple one-step mechanism in the absence of complications.

**Equilibrium Constant for the Reaction between  $\text{NNPE}_H$  and Hydroxide Ion in Water/Acetonitrile (50/50 vol %).** To estimate the equilibrium constant for  $\text{NNPE}_H$  (0.05 mM) in

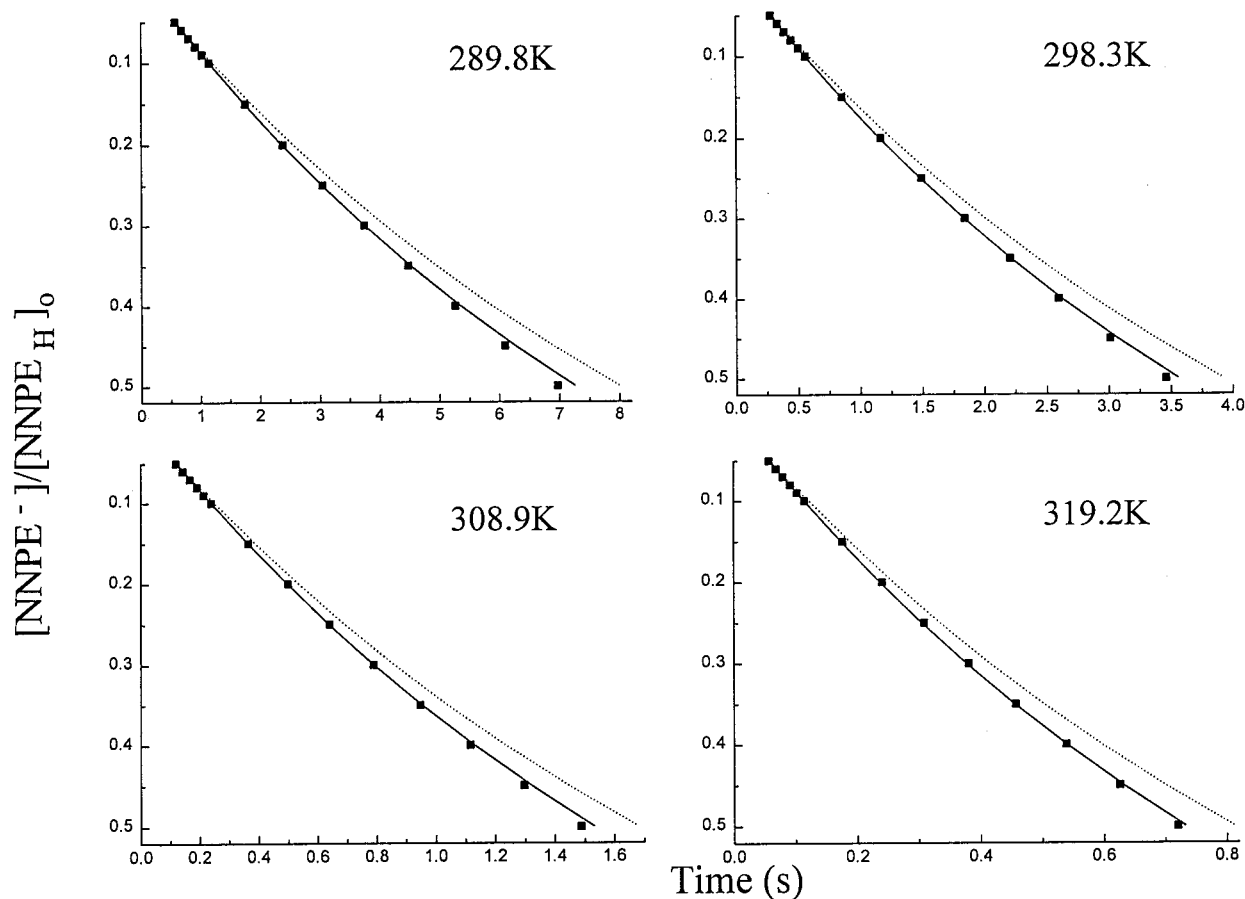


**Figure 3.** Extent of reaction–time profiles for the reactions of NNPE<sub>H</sub> (0.1 mM) with hydroxide ion (2.0 mM) at different temperatures: experimental data, solid squares; theoretical data for the 1-step mechanism, dashed lines; theoretical data for the 2-step mechanism, solid lines.

water/acetonitrile (50/50 vol %), the absorbance at 398 nm was recorded as a function of hydroxide concentration in the range from 0.05 to 1.5 mM. Conversion to NNPE<sup>-</sup> was complete, within experimental error, at [OH<sup>-</sup>] equal to 0.1 mM or greater. An experiment under the same conditions but with water/methanol (50/50 vol %) as solvent required [OH<sup>-</sup>] of 0.2 mM or greater to affect complete conversion to NNPE<sup>-</sup>. Since the p*K*<sub>a</sub> of NNPE<sub>H</sub> is equal to 7.5 in the latter solvent system, we conclude that it is no greater than 7.5 in water/acetonitrile (50/50 vol %) and that the equilibrium constant for the reaction with hydroxide ion is  $> 10^8$ .

**Estimation of Errors in Rate Constant Derived from the Fitting Procedure.** Six replicate experiments (each involving eight stopped-flow injections) were carried out on the reactions of both NNPE<sub>H</sub> (0.1 mM) and NNPE<sub>D</sub> (0.1 mM) with hydroxide ion (2.0 mM) in water/acetonitrile (50/50 vol %) at 298.3 K. The mean values of  $t_{\text{exp}}^{\text{H}}$  ( $M^{\text{H}}$ ) and  $t_{\text{exp}}^{\text{D}}$  ( $M^{\text{D}}$ ) were taken as the average values of the 48 data points. For each  $M^{\text{H}}$  (or  $M^{\text{D}}$ ) a standard deviation from the mean  $F^{\text{H}}$  (or  $F^{\text{D}}$ ) was recorded. For example, the mean values for extent of reaction equal to 0.05,  $M^{\text{H}}_{0.05}$  and  $M^{\text{D}}_{0.05}$ , have the associated standard deviations  $F^{\text{H}}_{0.05}$  and  $F^{\text{D}}_{0.05}$ . The appropriate mean values and associated standard deviations were evaluated for all extent of reactions in the data files. The standard deviations averaged about 2% for the NNPE<sub>H</sub> data and about 4% for the NNPE<sub>D</sub> data. The mean values,  $M^{\text{H}}$  and  $M^{\text{D}}$ , were used in the input data file to determine the best fit of the extent of reaction–time experimental data to theoretical data for mechanism 3. These rate constants are given in the first row of Table 5.

To determine the effect that the experimental error has on the rate constants derived by using the fitting procedure, we

either added or subtracted the appropriate  $F^{\text{H}}$  or  $F^{\text{D}}$  to the  $M^{\text{H}}$  or  $M^{\text{D}}$  using all possible combinations. The adjusted extent of reaction–time data files were then used as input for the fitting procedure and the best fit values of the rate constants were obtained. The values of  $k_{\text{app}}^{\text{H}}$  and  $k_{\text{app}}^{\text{D}}$  corresponding to the adjusted data were also determined. These results are summarized in Table 5. The deviations (in parentheses) from the rate constants derived from the mean values (row 1) are generally less than 5% but in the extreme cases are of the order of 10%. This suggests that the maximum errors in rate constants obtained by using the mean values of  $t_{\text{exp}}^{\text{H}}$  and  $t_{\text{exp}}^{\text{D}}$  are less than 10% of the mean values.

## Discussion

The proton-transfer reactions of nitroalkanes have received a great deal of attention in the past half-century.<sup>1–25</sup> They are moderately strong C–H acids and the conjugate bases are often long-lived which coupled with strong absorbance bands in the visible region renders the kinetics readily studied by conventional techniques. The question of quantum mechanical tunneling during cleavage of the C–H bond in these compounds has been the topic of much discussion. The controversy,<sup>7,8,12,14,23</sup> referred to earlier, arising from the reports of very large deuterium KIE in these reactions, left some uncertainty regarding the importance of tunneling in the proton-transfer reactions. For example, the very large values reported for the reactions of NPNM with TMG<sup>7,8</sup> have been shown to be incorrect<sup>12,14,23</sup> but very large deuterium KIE for reactions of trinitrotoluene with organic bases<sup>16,18</sup> have gone unchallenged.<sup>29</sup>

The primary objective of our study of the proton transfer reactions of nitroalkanes was to determine whether the reactions

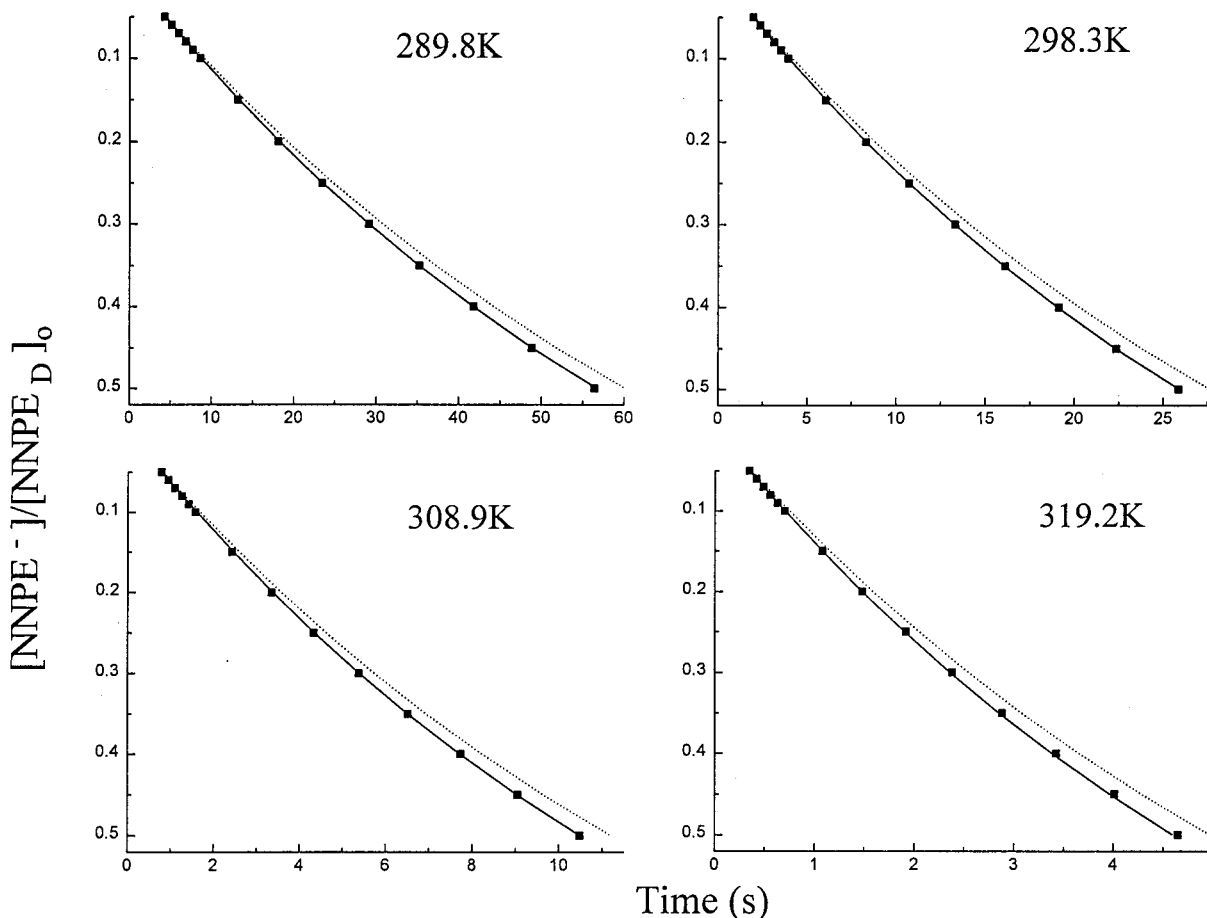


**Figure 4.** Extent of reaction–time profiles for the reactions of NNPE<sub>D</sub> (0.1 mM) with hydroxide ion (2.0 mM) at different temperatures: experimental data, solid squares; theoretical data for the 1-step mechanism, dashed lines; theoretical data for the 2-step mechanism, solid lines.

**Table 2.** Rate Constants for the Reactions of NNPE<sub>H(D)</sub> (0.1 mM) + NaOH (2.0 mM) in Water/Acetonitrile (50/50 vol %) at Different Temperatures<sup>a</sup>

<i>T</i> (K)	$k_{app}^H$	$k_{app}^D$	$k_f$	$k_p^H$	$k_p^D$	$k_b$	KIE <sub>app</sub>	KIE <sub>real</sub>
288.8	49.0	6.38	66.9	11.5	0.436	4.20	7.51–8.10	26.0
298.3	99.8	13.9	139	28.2	1.23	11.1	7.05–7.48	22.9
308.9	232	34.4	338	55.4	2.87	25.3	6.58–7.04	19.3
319.2	485	78.2	721	132	7.81	64.2	6.07–6.46	16.9

<sup>a</sup> Units: second-order rate constants ( $k_{app}^H$ ,  $k_{app}^D$ ,  $k_f$ ) are in M<sup>-1</sup> s<sup>-1</sup> and first-order rate constants ( $k_p^H$ ,  $k_p^D$ ,  $k_b$ ) are in s<sup>-1</sup>.

take place by the simple single-step mechanism 2 or if kinetically significant intermediates are formed in a 2-step mechanism 3. The key to distinguishing the 2-step mechanism from the simple single-step mechanism lies in the time period before the former achieves steady state.<sup>26</sup> In this time period, extent of reaction–time profiles for the 2-step mechanism differ significantly from those predicted for the 1-step mechanism. Also, KIE<sub>app</sub> for the single-step mechanism are independent of the extent of reaction while those for the 2-step mechanism may vary significantly. To achieve our objective it was necessary to choose reactants and conditions such that the proton-transfer reaction lies very far toward products to eliminate the complications arising from H/D exchange. The proton-

transfer reactions between NNPE<sub>H(D)</sub> and hydroxide ion in water/acetonitrile (50/50 vol %) fulfill the necessary requirements.

All of our experimental results for the reactions of NNPE<sub>H(D)</sub> with hydroxide ion in water/acetonitrile (50/50 vol %) deviate significantly from those predicted for the 1-step mechanism. The extent of reaction–time profiles illustrated in Figures 1–4 are inconsistent with the single-step mechanism. In all cases KIE<sub>app</sub> were observed to increase significantly with the extent of reaction in the 0.05 to 0.50 range, which is also inconsistent with the single-step mechanism.

On the other hand, excellent fits of experimental to theoretical data for the 2-step mechanism were obtained for extent of reaction–time profiles for reactions of NNPE<sub>H</sub> (Figure 1) and NNPE<sub>D</sub> (Figure 2) in which the hydroxide ion concentration was varied from 0.5 to 5.0 mM. Similar results were obtained for reactions in which the temperature was varied from 288.8 to 319.2 K (Figures 3 and 4). All experimental ( $t_{0.5}/t_{0.05}$ )<sub>H(D)</sub> were significantly lower than the theoretical value for the single-step mechanism (Figure 1–4). This is particularly important in considering the possible effect of the reverse reactions and H/D exchange on extent of reaction–time profiles. For the simple reversible reaction 1 under the conditions used in this study, neither reversibility nor H/D exchange could give rise to the observed deviations from simple mechanism behavior. In fact, when these complications exist the ( $t_{0.5}/t_{0.05}$ )<sub>H(D)</sub> are affected in the opposite manner, i.e. they become greater (Table 3) rather than smaller than 13.5 as observed. Furthermore, the theoretical data in Table 3 show that the complications due to either of these factors will only be of importance under our conditions

(28) Steinfeld, J. I.; Francisco, J. S.; Hase, W. M. *Chemical Kinetics and Dynamics*; Prentice Hall: Upper Saddle River, NJ, 1999; Chapter 2.

(29) Although arguments were presented<sup>16,18</sup> to exclude the possibility that H/D exchange is responsible for the very large deuterium KIE reported, our calculations assuming equilibrium 1 using their equilibrium constants predict KIE<sub>app</sub> very heavily influenced by exchange. Our results on these reactions will be reported.

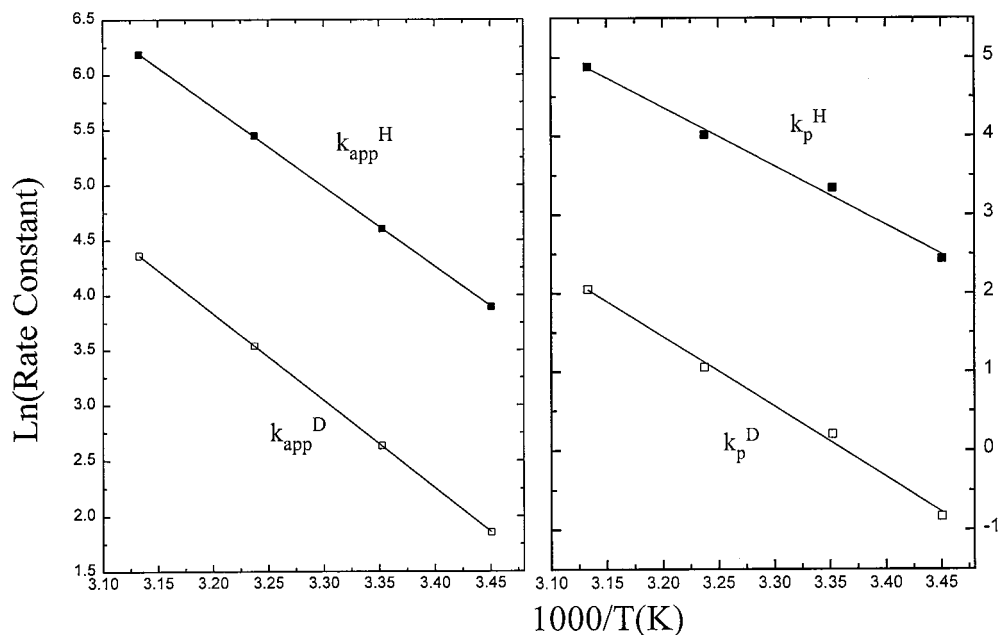


**Figure 5.** Arrhenius plots for the reactions of NNPE<sub>H</sub> (solid squares) and NNPE<sub>D</sub> (open squares) based on apparent rate constants ( $k_{app}^{H(D)}$ ) and rate constants for the proton ( $k_p^H$ ) and deuteron ( $k_p^D$ ) transfer steps.

**Table 3.** The Effect of the Magnitude of the Equilibrium Constant on the Extent of Reaction–Time Profiles of Reversible Proton-Transfer Reactions<sup>a</sup>

$K_{equil}$	$(t_{0.50}/t_{0.05})_H$	$(t_{0.50}/t_{0.05})_D$	$10^4[A^-]_{equil}/M$
$1.67 \times 10^4$	20.6	28.9	0.597
$2.00 \times 10^4$	18.6	25.0	0.640
$2.50 \times 10^4$	17.1	21.9	0.689
$3.30 \times 10^4$	15.9	19.3	0.745
$5.00 \times 10^4$	15.0	17.1	0.816
$1.00 \times 10^5$	14.2	15.2	0.898
$1.00 \times 10^6$	13.6	13.7	0.989
$1.00 \times 10^7$	13.5	13.5	0.999
$1.00 \times 10^8$	13.5	13.5	0.9999
$1.00 \times 10^9$	13.5	13.5	0.99999

<sup>a</sup> Theoretical data for equilibrium 1;  $k_f^H = 100 \text{ M}^{-1} \text{ s}^{-1}$ ,  $k_f^D = 10 \text{ M}^{-1} \text{ s}^{-1}$ ,  $k_b^H = k_b^D$ ,  $[HA]_0 = 0.0001$ ,  $[B]_0 = 0.005$ .

**Table 4.** The Effect of the Magnitudes of the Rate Constants of Nonproductive Equilibria on the Extent of Reaction–Time Profiles of Proton-Transfer Reactions<sup>a</sup>

$k_b(\text{nonproductive})/\text{s}^{-1}$	$(t_{0.50}/t_{0.05})$ when $k_f(\text{nonproductive})/\text{M}^{-1} \text{ s}^{-1}$ is equal to			
	0.10	0.33	0.60	1.00
0.0001	14.2	15.9	19.3	46.9
0.0010	14.1	15.8	19.0	31.7
0.0100	14.0	15.2	16.9	20.2
0.1000	13.6	13.9	14.1	14.5
1.0000	13.6	13.6	13.6	13.6

<sup>a</sup> Theoretical data for an irreversible proton-transfer reaction;  $k_f(\text{productive}) = 1 \text{ M}^{-1} \text{ s}^{-1}$ ,  $[HA]_0 = 0.0001 \text{ M}$ ,  $[B]_0 = 0.01 \text{ M}$ .

when the equilibrium constant is  $< 10^6$ , which is at least 2 orders of magnitude lower than  $K_{equil}$  under the reaction conditions.

The conclusion that cannot be avoided from the discussion in the previous paragraphs is that the kinetic data are inconsistent with the simple single-step proton-transfer mechanism and that the 2-step mechanism involving a kinetically significant intermediate consistently predicts extent of reaction–time profiles that match closely with the experimental data.

The rate constants derived at 298.3 K result in  $KIE_{real}$  equal to  $22.4 \pm 1.0$ . This value is clearly larger than expected in the absence of quantum mechanical tunneling. Bell<sup>30,31</sup> suggests the following values of parameters to be characteristic of processes

involving significant proton tunneling:  $k^H/k^D > 10$ ,  $E_a^D - E_a^H > 1.35 \text{ kcal/mol}$ , and the ratio of Arrhenius preexponential factors ( $A^D/A^H$ )  $> 1.4$ . The Arrhenius parameters summarized in Table 6 were derived from both the apparent rate constants and those obtained by the fitting procedure. The activation parameters for the proton and deuteron transfer steps, from the temperature dependence of  $k_p^H$  and  $k_p^D$ , provide additional evidence for proton tunneling. The activation energy difference ( $E_a^D - E_a^H = 2.80$ ) and the ratio of preexponential factors ( $A^D/A^H = 4.95$ ) derived from  $k_p^H$  and  $k_p^D$  are clearly in the range expected for significant proton tunneling.<sup>30,31</sup> Activation parameters derived from the apparent rate constants, on the other hand, are close to the semiclassical limits and do not provide evidence for tunneling.

The intermediate in the reaction is most likely a donor/acceptor complex between hydroxide ion and the electron deficient  $\pi$ -system of NNPE<sub>H(D)</sub>. An alternative possibility for the structure of the complex involves a C–H $\cdots$ O hydrogen bond from NNPE<sub>H(D)</sub> to hydroxide ion. Although similar hydrogen bonds are believed to be of importance in the gas phase,<sup>32</sup> they would appear to be highly unlikely in the strongly hydrogen bonding aqueous solvent. The data in Table 4 show that the formation of an unreactive NNPE/OH<sup>-</sup> complex is not responsible for the deviations from the simple single-step mechanism. The nonproductive equilibrium causes  $(t_{0.50}/t_{0.05})$  to deviate in the opposite manner than is experimentally observed. A possibility which cannot be ruled out is that a Meisenheimer complex<sup>33</sup> is formed in the first step of the reaction which then eliminates water in the product-forming step.

A preassociation mechanism for proton transfer is not new. A three-step mechanism for proton transfer—(i) the formation of an encounter complex, (ii) proton transfer to form a new complex, and (iii) separation to products—is generally accepted for the combination of hydronium ion with anions from the work of Eigen.<sup>34</sup> Preassociation in general acid catalysis<sup>35</sup> has long

(30) Bell, R. P. *Trans. Faraday Soc.* **1959**, *55*, 1.

(31) Bell, R. P. *The Tunnel Effect in Chemistry*; Chapman and Hall: London, 1980.

(32) Turi, L.; Dannenberg, J. J. *J. Phys. Chem.* **1995**, *99*, 639.

(33) Minch, M. J.; Giaccio, M.; Wolff, R. *J. Am. Chem. Soc.* **1975**, *97*, 3766.

**Table 5.** Effect of Experimental Error on Errors in the Rate Constants Derived Using the Fitting Procedure<sup>a,b</sup>

$t_{\text{exp}}^{\text{H}}$	$t_{\text{exp}}^{\text{D}}$	$k_{\text{app}}^{\text{H}}$	$k_{\text{app}}^{\text{D}}$	$k_{\text{f}}/\text{M}^{-1}\text{s}^{-1}$	$k_{\text{p}}^{\text{H}}/\text{s}^{-1}$	$k_{\text{p}}^{\text{D}}/\text{s}^{-1}$	$k_{\text{b}}/\text{s}^{-1}$	KIE <sub>real</sub>
$M^{\text{H}}$	$M^{\text{D}}$	99.8 (0.0)	13.9 (0.0)	139 (0.0)	28.2 (0.0)	1.23 (0.0)	11.1 (0.0)	22.9 (0.0)
$M^{\text{H}} + \sigma^{\text{H}}$	$M^{\text{D}}$	97.5 (2.3)	13.9 (0.0)	137 (1.4)	28.0 (0.7)	1.28 (4.1)	11.4 (2.7)	21.9 (4.4)
$M^{\text{H}}$	$M^{\text{D}} + \sigma^{\text{D}}$	99.8 (0.0)	13.3 (4.3)	146 (5.0)	28.5 (1.1)	1.32 (7.3)	13.2 (18.9)	21.6 (5.7)
$M^{\text{H}} + \sigma^{\text{H}}$	$M^{\text{D}} + \sigma^{\text{D}}$	97.5 (2.3)	13. (4.3)	137 (1.4)	29.2 (3.6)	1.27 (3.3)	11.9 (7.2)	23.0 (0.4)
$M^{\text{H}} - \sigma^{\text{H}}$	$M^{\text{D}} - \sigma^{\text{D}}$	102 (2.2)	14.5 (4.3)	142 (2.2)	26.9 (4.6)	1.22 (0.8)	10.8 (2.7)	22.1 (3.5)
$M^{\text{H}} - \sigma^{\text{H}}$	$M^{\text{D}} + \sigma^{\text{D}}$	102 (2.2)	13.3 (4.3)	141 (1.4)	27.5 (2.5)	1.14 (7.3)	11.0 (0.9)	24.1 (5.2)
$M^{\text{H}} + \sigma^{\text{H}}$	$M^{\text{D}} - \sigma^{\text{D}}$	97.5 (2.3)	14.5 (4.3)	138 (0.7)	28.6 (1.4)	1.38 (1.4)	11.9 (7.2)	20.8 (9.2)

<sup>a</sup> Definition of symbols used:  $M^{\text{H}}$  = average values of  $t_{\text{exp}}^{\text{H}}$ ;  $M^{\text{D}}$  = average values of  $t_{\text{exp}}^{\text{D}}$ ;  $\sigma^{\text{H}}$  = standard deviations in data for NNPE<sub>H</sub>;  $\sigma^{\text{D}}$  = standard deviations in data for NNPE<sub>D</sub>. <sup>b</sup> Numbers in parentheses are the percentage deviations from the best fit values ( $M^{\text{H}}$  and  $M^{\text{D}}$  data sets).

**Table 6.** Arrhenius Parameters for Proton- and Deuteron-Transfer Reactions of NNPE<sub>H(D)}</sub> (0.1 mM) + NaOH (2.0 mM) in Water/Acetonitrile (50/50 vol %)

	apparent <sup>a</sup>		real <sup>b</sup>			
	H	D	H	D		
$E_{\text{a}}$ (kcal/mol)	14.4	15.7	14.9	17.7		
$E_{\text{a}}^{\text{D}} - E_{\text{a}}^{\text{H}}$ (kcal/mol)	1.30		2.80			
$A$ ( $10^{12}$ )	3.32	4.17	1.86	9.20		
$A^{\text{D}}/A^{\text{H}}$	1.26		4.95			

<sup>a</sup> Derived from  $k_{\text{app}}^{\text{H}}$  and  $k_{\text{app}}^{\text{D}}$ . <sup>b</sup> Derived from  $k_{\text{p}}^{\text{H}}$  and  $k_{\text{p}}^{\text{D}}$ .

been advocated by Jencks and others. The pre-steady-state kinetic studies reported here allowed us to resolve the kinetics of the 2-step mechanism and evaluate the microscopic rate constants for the proton-transfer reaction between NNPE<sub>H(D)}</sub> and hydroxide ion.

## Conclusions

Kinetic data for the reaction between NNPE<sub>H(D)}</sub> with hydroxide ion in water/acetonitrile (50/50 vol %) are inconsistent with the simple single-step mechanism. On the other hand, excellent fits of experimental extent of reaction–time profiles to theoretical data for the 2-step mechanism involving a kinetically significant intermediate complex were observed under all conditions studied. A consistent set of rate constants for the reactions of both NNPE<sub>H</sub> and NNPE<sub>D</sub> were derived for hydroxide concentrations ranging from 0.5 to 5.0 mM. The resolution of the apparent rate constants into the microscopic rate constants,  $k_{\text{f}}$ ,  $k_{\text{b}}$ ,  $k_{\text{p}}^{\text{H}}$ , and  $k_{\text{p}}^{\text{D}}$ , gives access to a KIE<sub>real</sub> (equal to 22) that is considerably larger than the extent of reaction-dependent KIE<sub>app</sub> (ranging from 7.02 to 7.53) and is consistent with a considerable degree of proton tunneling. The Arrhenius parameters also provide evidence for tunneling.

The most important feature of this reaction which provided the opportunity to resolve the apparent rate constants into the microscopic rate constants for the individual steps in the complex mechanism is that steady state is not reached until late in the first half-life. In the time period before steady-state is reached, KIE<sub>app</sub> were observed to increase with increasing extent of reaction which contributes to the ease of resolution of the kinetics.

## Experimental Section

**Materials.** NNPE<sub>H</sub> was prepared by using a modification of the literature<sup>21</sup> procedure (50% H<sub>2</sub>O<sub>2</sub> was substituted for 90% H<sub>2</sub>O<sub>2</sub>). NNPE<sub>D</sub> was prepared by hydrogen/deuterium exchange as reported earlier.<sup>24</sup> Acetonitrile (Aldrich, HPLC Grade) was distilled twice (collecting the middle fraction) after refluxing over P<sub>2</sub>O<sub>5</sub> for 24 h. Distilled water was further purified by passing through a Barnsted Nanopure Water System. Concentrations of freshly prepared sodium hydroxide solutions were determined by titration with standard oxalic acid solutions.

**Absorbance Measurements.** Optical absorbance measurements at 398 nm on NNPE<sup>-</sup> in water/acetonitrile (50/50 vol %) were carried out by allowing NNPE<sub>H</sub> (0.05 mM) to react with hydroxide ion (0.05 to 1.50 mM) with use of a Hewlett-Packard 8452A Diode Array spectrophotometer.

**Data Collection.** The kinetic measurements were carried out on a Hi-Tech Scientific SF-61 stopped flow spectrophotometer with a Techne Flow Cooler FC-200 thermostat to control the temperature of the cell block within  $\pm 0.2$  °C. Data, about 2000 points over the first half-life, were collected under both pseudo-first-order and second-order conditions for the reaction of NNPE<sub>H(D)}</sub> with hydroxide ion (0.5–5.0 mM) in water/acetonitrile (50/50 vol %).

**Data Manipulation.** The 2000 data points for each kinetic run were smoothed by the least-squares procedure of Savitzky and Golay.<sup>36</sup> The background absorbance was then subtracted and the absorbance–time data were converted to extent of reaction–time data ( $[A^-]/[HA]_0$  vs  $t$ ) and the times necessary for the ratio to equal to 0.05 to 0.50 (at 0.05 intervals) were determined. The latter were collected in data files for import into the program for fitting of experimental to theoretical data.

**Data Fitting Procedure.** The procedure for fitting experimental to theoretical derivative cyclic voltammetry data was described in detail in ref 26. The published procedure is directly applicable to the stopped-flow kinetic data reported here. Therefore, the procedure will only be described briefly.

The experimental input includes  $k_{\text{app}}^{\text{H}}$  and  $k_{\text{app}}^{\text{D}}$  as well as the extent of reaction–time data files for HA and DA. The procedure involves determining deviations between experimental ( $t_{\text{exp}}^{\text{H}}$  and  $t_{\text{exp}}^{\text{D}}$ ) times to reach the specific extent of reaction from 0.05 to 0.50 and those from theoretical data for the 2-step mechanism ( $t_{\text{sim}}^{\text{H}}$  and  $t_{\text{sim}}^{\text{D}}$ ). The differences in experimental and theoretical times are determined at each extent of reaction and  $\Sigma_{\text{H(D)}}^2$  (equal to  $(t_{\text{exp}}^{\text{H(D)}} - t_{\text{sim}}^{\text{H(D)}})^2/t_{\text{sim}}$ ) are summed for the entire range (0.05 to 0.50). The same procedure is carried out for KIE<sub>app</sub> (equal to  $t_{\text{exp}}^{\text{D}}/t_{\text{exp}}^{\text{H}}$  at the particular extent of reaction). For each experimental to theoretical data comparison the procedure results in three measures of the deviations between the two data sets,  $\Sigma_{\text{H}}$ ,  $\Sigma_{\text{D}}$ , and  $\Sigma_{\text{KIE}}$ . The range of  $k_{\text{f}}$  over which significant deviations from the single-step mechanisms can be observed is limited from about  $k_{\text{app}}^{\text{H}}$  to  $11(k_{\text{app}}^{\text{H}})$ .<sup>26</sup> With this in mind we typically select about ten  $k_{\text{f}}$  values over this range, starting at 1.1 ( $k_{\text{app}}^{\text{H}}$ ), and determine what values of the other rate constants ( $k_{\text{b}}$ ,  $k_{\text{p}}^{\text{H}}$ , and  $k_{\text{p}}^{\text{D}}$ ) give the best fit for that particular  $k_{\text{f}}$  value. This is accomplished by systematically varying  $k_{\text{p}}^{\text{H}}$  and adjusting ( $k_{\text{b}}$  and  $k_{\text{p}}^{\text{D}}$ ) to conform to eqs 5–7. For each  $k_{\text{f}}$  three series of fitting parameters, corresponding to  $\Sigma_{\text{H}}$ ,  $\Sigma_{\text{D}}$ , and  $\Sigma_{\text{KIE}}$ , as a function of  $k_{\text{p}}^{\text{H}}$  are obtained.  $\Sigma_{\text{KIE}}$  are used directly in the data fit, while  $\Sigma_{\text{H}}$  and  $\Sigma_{\text{D}}$  are monitored to ensure the quality of the fits to the two response curves. Plots of  $\Sigma_{\text{KIE}}$  vs  $k_{\text{p}}^{\text{H}}$  are parabola-like curves with minima that reflect the best fit for that  $k_{\text{f}}$  value. We then have a series of fitting parameters at the minimum,  $(\Sigma_{\text{KIE}})_{\text{min}}$ , as a function of  $k_{\text{f}}$ . A plot of  $k_{\text{f}}$  vs  $(\Sigma_{\text{KIE}})_{\text{min}}$  is, again, parabola-like with a minimum that reflects the best value of  $k_{\text{f}}$ . To arrive at overall best fits of data it is necessary to carry out several iterations of the fitting procedure.

**Acknowledgment.** We acknowledge the donors of the Petroleum Research Fund, administered by the American Chemical Society, as well as the National Science Foundation (CHE-970835 and CHE-0074405), for support of this work.

JA0036070

(34) Eigen, M. *Angew. Chem., Int. Ed. Engl.* **1964**, *3*, 1.

(35) Jencks, J. P. *Acc. Chem. Res.* **1980**, *13*, 161.

(36) Savitzky, A.; Golay, M. *Anal. Chem.* **1964**, *36*, 1627.